Investigation of CMB Power Spectra Phase Shifts

Brigid Mulroe
Fordham University, Bronx, NY, 10458

Lloyd Knox, Zhen Pan
University of California, Davis, CA, 95616

ABSTRACT

Analytical descriptions of anisotropies in the Cosmic Microwave Background predict peaks of the temperature power spectrum to line up with troughs in the polarization power spectrum, but new data from the Planck collaboration show a small but significant phase shift from this expected alignment. We investigate two possible sources of this disparity: a phase shift between primordial perturbations of temperature and polarization, and differences in the way each perturbation projects into anisotropies on the sky. We find that both phenomena are present and affect the present-day anisotropies in ways not predicted by current analytical models.

1. Introduction

The Cosmic Microwave Background (CMB) is a major source of information for cosmologists. It consists of photons that last interacted with matter when the universe was around 300,000 years old, at a redshift of around 1100, so analysis of CMB observables can give us information about the very early universe. It can place limits on cosmological parameters and provide tests for theories of structure formation, helping to explain how our universe originated and evolved to its present state. For these reasons, understanding the CMB in precise detail is very important. In this paper, we investigate the accuracy of analytical descriptions of CMB anisotropies by attempting to explain a phase shift which they do not predict.

At redshifts greater than 1100, the high energy density of the universe meant that matter was ionized. Free electrons interacted with both photons (in Thomson scattering) and protons (by the electromagnetic force) and thus coupled light to baryons in what can be approximated as a fluid. As the universe expanded and cooled, the expansion rate outpaced the scattering rate, matter de-ionized, and light decoupled from the primordial fluid, freestreaming through space until the present day (neglecting reionization). The temperature of the CMB that we observe therefore indicates the temperature of the primordial fluid at the time of last scattering. This temperature is very nearly uniform at 2.725 K, indicating that the early universe was very smooth and homogeneous, but there are fluctuations of 10^{-5} K across the sky, reflecting small perturbations in the primordial fluid.

In addition to temperature fluctuations, the CMB exhibits irregularities in its polarization. Light is polarized by Coulomb scattering depending on the angle at which it scatters. If the temperature of photons in the primordial fluid in all directions was uniform, the combination of light scattered at all angles into a single direction would give net zero polarization. But if photons approaching an electron at 90°separation from each other have different intensities, the polarization state of the higher intensity direction will dominate and the outgoing light will be polarized. Therefore, a quadrupole anisotropy in the temperature of the primordial fluid sources an anisotropy in polarization. The quadrupole only arises around the time of decoupling, when the tight coupling approximation starts to break down, and is much weaker than the monopole and dipole. For this

reason polarization anisotropies are much smaller and harder to detect today. The first detailed description of the polarization power spectrum was released by the Planck Collaboration (2015) earlier this year.

As we will see, mathematical analysis indicates that the monopole and quadrupole perturbations are out of phase with each other, so we would expect the observed temperature and polarization anisotropy spectra to be out of phase as well, with the peaks of one lining up with the troughs of the other. This turns out to be roughly true, but as new data from the Planck collaboration show, there is a slight phase shift. We hypothesize two possible sources for this phase shift: first, it could be a reflection of a phase shift between temperature and polarization perturbations in the primordial plasma, due to higher order terms ignored in the tight coupling approximation. It could also arise from the projection of perturbations into anisotropies on the sky today, if temperature and polarization perturbations project differently. In this paper, we analyze simulations of both early perturbations and current spectra in an attempt to specify the mechanism producing the phase shift.

2. Mathematical Descriptions of CMB Anisotropies

CMB anisotropies are usually represented as $\Theta_T = \frac{\Delta T}{T}$ and $\Theta_P = \frac{\Delta E}{E}$ where E is a polarization eigenstate of the radiation. The anisotropy of photons with momentum $\hat{p}$ at location $\vec{x}$ and conformal time η can be indicated by $\Theta(\vec{x}, \hat{p}, \eta)$, but it is more often represented as its Fourier transform $\Theta(\vec{k}, \hat{p}, \eta)$. This representation is useful because the perturbations are small enough to be treated with linear perturbation theory, where separate Fourier modes evolve separately. Another common transformation is the Legendre decomposition:

$$\Theta_l(\vec{k}, \eta) = \frac{1}{-i^l} \int_{-1}^{1} \frac{d\mu}{2} P_l(\mu) \Theta(\vec{k}, \hat{p}, \eta) \quad (1)$$

Where $\mu = \frac{\vec{k} \cdot \hat{p}}{k}$. Each Θ_l is a multipole moment of the anisotropy and goes through l oscillations over one complete rotation. It is useful to express anisotropies in terms of multipoles when describing their evolution in time, and this is the most common way to express CMB anisotropies.

Any mathematical analysis of anisotropies must begin with the Boltzmann and Einstein equations, a set of nine coupled differential equations describing the behavior of photons, baryons, neutrinos, and cold dark matter. To be solved exactly, these equations must be expanded into a hierarchy of multipole moments to a chosen l_{max} and evolved numerically up to the present. Analytical approximations, however, are helpful for illuminating the underlying physics giving rise to anisotropies. An analytical approach introduced by Hu & Sugiyama (1995) and expanded to include polarization by Zaldarriaga & Harari (1995) looks at the evolution of temperature perturbations in two regimes: the tight coupling regime, where photons and baryons are approximated as an oscillating fluid; and freestreaming, where perturbations are projected through space with no further physical evolution. This approach is described in more detail below.

The Boltzmann equations for photons and baryons, derived in Chapter 4 of Dodelson (2003), read

$$\dot{\Theta}_T + ik\mu(\Theta_T + \Psi) = -\dot{\Phi} - \dot{\tau}[\Theta_{T0} - \Theta_T + \mu v_b - \frac{1}{2} P_2(\mu)\Pi] \quad (2)$$

$$\dot{\Theta}_P + ik\mu\Theta_P = -\dot{\tau}[-\Theta_P + \frac{1}{2}(1 - P_2(\mu))\Pi] \quad (3)$$

$$\Pi = \Theta_{T2} + \Theta_{P2} + \Theta_{P0} \quad (4)$$

$$\dot{\delta_b} + ikv_b = -3\dot{\Phi} \quad (5)$$

$$\dot{v_b} + \frac{\dot{a}}{a} v_b = -ik\Psi + \frac{\dot{\tau}}{R}[v_b + 3i\Theta_{T1}] \quad (6)$$

where Θ refers to the Fourier transformed anisotropy, d_b and v_b are the baryon density and velocity, and $\dot{\tau}$ is the scattering rate or differential optical depth. Similar equations describe neutrinos and cold dark matter, but these components will only be considered through their gravitational effects on the metric perturbations Φ and Ψ. We can expand the Boltzmann equations in powers of $\dot{\tau}^{-1}$, which will be small when $\dot{\tau}$ is large, as it is in the tight coupling limit. To first order, and written in terms of multipole moments, this gives the

equations

$$\Theta_{T1} = \frac{iv_b}{3} = \frac{-1}{k}(\dot{\Theta}_{T0} + \dot{\Phi}) \quad (7)$$

$$\Theta_{T2} = \frac{8}{15}\dot{\tau}^{-1}k\Theta_{T1} \quad (8)$$

$$\Theta_{P2} = \frac{1}{5}\Theta_{P0} = \frac{1}{4}\Theta_{T2} \quad (9)$$

$$\Theta_{(T,P)l} = 0, l \geq 3 \quad (10)$$

Note that equations (7)-(9) imply that Θ_{T1}, Θ_{T2}, Θ_{P0}, and Θ_{P2} (and therefore Π from equation (4)) are all proportional to the derivative of the effective temperature monopole. Also from our first order expansion, we obtain for the photon temperature the equation of a forced, damped oscillator:

$$\ddot{\Theta}_{T0} + \frac{\dot{a}}{a}\frac{R}{1+R}\dot{\Theta}_{T0} + k^2c_s^2\Theta_{T0} = -\frac{k^2}{3}\Psi - \frac{\dot{a}}{a}\dot{\Phi} - \ddot{\Phi} \quad (11)$$

where $c_s = \frac{1}{3(1+R)}$ is the sound speed of the fluid, giving a sound horizon $r_s(\eta) = \int_0^\eta c_s d\eta'$. The solution to this equation is

$$\Theta_{T0}(\eta) + \Phi(\eta) = [\Theta_{T0}(0) + \Phi(0)]\cos(kr_s) + \frac{k}{\sqrt{3}}\int_0^\eta [\Phi(\eta') - \Psi(\eta')]\sin[kr_s(\eta) - kr_s(\eta')] \quad (12)$$

To account for diffusion damping on smaller scales, the entire expression can be multiplied by a factor of $e^{-[k/k_D(\eta)]^2}$. If we expect the first term in this solution to dominate, we will expect the perturbations to oscillate with peaks at $k_n = n\pi/r_s$.

Next is the freestreaming projection from the time of decoupling to the current time. Going back to the photon Boltzmann equations, we can solve them for the perturbations today:

$$[\Theta_T + \Psi](\eta_0, \mu) = \int_0^{\eta_0} d\eta[(\Theta_{T0} + \Psi - i\mu v_b)\dot{\tau} - \dot{\Phi} + \dot{\Psi}] * e^{-\tau(\eta,\eta_0)}e^{ik\mu(\eta-\eta_0)} \quad (13)$$

$$= \int_0^{\eta_0} d\eta g(\eta)(\Theta_{T0} + \Psi)e^{ik\mu(\eta-\eta_0)} + \int_0^{\eta_0} d\eta g(\eta)(-i\mu v_b)e^{ik\mu(\eta-\eta_0)} + \int_0^{\eta_0} d\eta(\dot{\Psi} - \dot{\Phi})e^{-\tau(\eta,\eta_0)}e^{ik\mu(\eta-\eta_0)} \quad (14)$$

$$\Theta_P(\eta_0, \mu) = \frac{3}{4}(1-\mu^2)\int_0^{\eta_0} d\eta g(\eta)\Pi e^{ik\mu(\eta-\eta_0)} \quad (15)$$

For the temperature perturbations, we will focus only on the first line of equation (15). The quantity $g(\eta) = \dot{\tau}(\eta)e^{-\tau(\eta)}$, called the visibility function, indicates the probability that a photon last scattered at η. The visibility function peaks sharply at η_*, the time of decoupling, and Hu & Sugiyama approximate it as a delta function. This allows them to replace the first integral with the values of the perturbations at η_* obtained with the tight coupling solution. For the temperature perturbations, this means cosine-like oscillations with a period of about kr_s. The polarization perturbation Π, which as we noted above is proportional to the derivative of the temperature monopole, should then oscillate at the same period but shifted by $\frac{\pi}{2}$.

This analytical approach is appealing for its clarity, but it loses some accuracy in assuming a sharp transition from tight coupling to freestreaming. Seljak & Zaldarriaga (1996) introduced a new formalism to allow perturbations to be accurately calculated without obscuring the underlying physics. They break the anisotropies into a source term, representing primordial perturbations, and a geometric term, representing projection into today's anisotropies. Each term can be calculated numerically, with much greater speed than the full set of Boltzmann equations, and then convolved together. The source terms are defined

$$S_T(k,\eta) = g(\eta)\left[\Theta_0(k,\eta) + \Psi(k,\eta) + \frac{\Pi}{4}\right] + \frac{d}{d\eta}\left(\frac{iv_b(k,\eta)g(\eta)}{k}\right) - \frac{3}{4k^2}\frac{d^2}{d\eta^2}[g(\eta)\Pi(\eta)] + e^{-\tau}[\dot{\Psi}(k,\eta) - \dot{\Phi}(k,\eta)] \quad (16)$$

$$S_P(k,\eta) = \frac{3}{4k^2}\frac{d^2}{d\eta^2}[g(\eta)\Pi(\eta)] + \frac{3}{4}g(\eta)\Pi(\eta) \quad (17)$$

We will again consider only the first term in the temperature source funcion. The anisotropies can then be written

$$\Theta_{T,P}(k,\eta_0) = \int_0^{\eta_0} d\eta e^{ik\mu(\eta-\eta_0)}S_{T,P}(k,\eta) \quad (18)$$

$$\Theta_{(T,P)l}(k,\eta_0) = \int_0^{\eta_0} d\eta S_{T,P}(k,\eta)j_l[kd_A(\eta)] \quad (19)$$

where $d_A(\eta)$ is called the angular diameter distance and in a flat universe is equal to $\eta - \eta_0$.

Remembering that the source terms of interest to us peak at $\eta = \eta_*$, we can say several things about Θ_l, sometimes called the transfer function. The spherical Bessel function $j_l(x)$ oscillates very quickly and peaks close to $x = l$, so Θ_l should exhibit a peak at an l correspondingly close to kd_A. The source term will produce an envelope behaving like the perturbations at recombination. See the last page for an illustration.

Finally, to relate these multipole anisotropies to our observations of the CMB, we can expand the observed anisotropy on the sky in spherical harmonics:

$$\Theta(\vec{x}, \hat{p}, \eta) = \sum_{l=1}^{\infty} \sum_{m=-l}^{l} a_{lm}(\vec{x}, \eta), Y_{lm}(\hat{p}) \qquad (20)$$

and we write the variance of the a_{lm}'s

$$\langle a_{lm} a^*_{l'm'} \rangle = \delta_{ll'} \delta_{mm'} C_l \qquad (21)$$

where the C_l's can be expressed in terms of the transfer functions and the matter power spectrum $P(k)$:

$$C_l = \frac{2}{\pi} \int_0^{\infty} dk k^2 P(k) \left| \frac{\Theta_l(k)}{\delta(k)} \right|^2 \qquad (22)$$

For a derivation, see Dodelson (2003), section 8.5.2. Because the transfer functions Θ_l contribute most near $l = kd_A$, when we square them and integrate over k, we expect to find peaks in l-space corresponding to both peaks and troughs in k-space. This is backed up by physical reasoning: for angular scales corresponding to wavenumbers at extrema of displacement when freestreaming begins, we will see strong patterns of oscillation across the sky.

We can therefore trace the phase shift between temperature and polarization through all the stages of evolution. If Θ_{T0} and Π are indeed harmonic oscillations with a phase shift of $\frac{\pi}{2}$ between them, this phase shift will be reflected exactly in the source terms $S_{T,P}$ and in the transfer functions $\Theta_{l(T,P)}$. When we convert Θ_l to C_l the period of oscillation is halved, so the effective phase shift is now π. This is the justification for our expectation that the peaks in one power spectrum will line up with the troughs in the other.

3. Problem and Hypotheses

Below are listed the locations of peaks and troughs in the temperature and polarization power spectra, as measured by the Planck Collaboration (2015). Not only do they not line up as we would expect them to from the physical and mathematical reasoning in the previous sections, but the phase shift between them (shown in Figure 2), as well as the spacing between peaks and troughs in each spectrum, change in nonuniform ways. Evidently, there are significant processes in the evolution of perturbations which lead to a phase shift, and which are not encompassed in the analytical descriptions in the previous section. The aim of this project was to identify these processes. Following the traditional breakdown of evolution into the tight coupling and freestreaming epochs, we

TT Spectrum		EE Spectrum	
		first peak:	137 ± 6
first peak:	220.0 ± 0.5	first trough:	197 ± 8
first trough:	415.5 ± 0.8	second peak:	397.2 ± 0.5
second peak:	537.5 ± 0.7	second trough:	525 ± 0.7
second trough:	676.1 ± 0.8	third peak:	690.8 ± 0.6
third peak:	810.8 ± 0.7	third trough:	832.8 ± 1.1
third trough:	997.7 ± 1.4	fourth peak:	992.1 ± 1.3
fourth peak:	1120.9 ± 1.0	fourth trough:	1153.9 ± 2.7
fourth trough:	1288.8 ± 1.6	fifth peak:	1296 ± 4

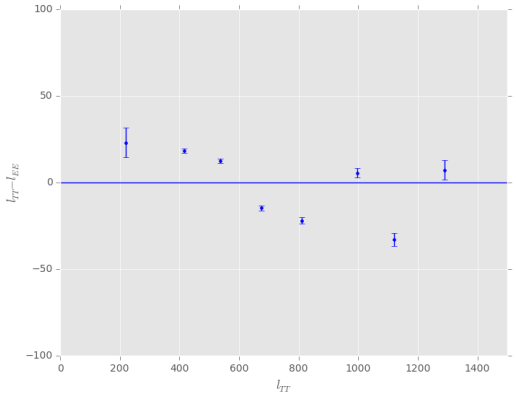

Fig. 1.— The distance between corresponding peaks and troughs in the temperature and polarization power spectra, which would be expected to fall very close together.

looked into each regime separately. First we asked whether a phase shift existed between the temperature and polarization perturbations near the time of decoupling, and then we asked whether each set of perturbations projected differently into today's anisotropies.

4. Methods

Our primary computation tool was CLASS, a code which numerically solves the Boltzmann and Einstein equations. CLASS uses several approximations in certain regions to reduce calculation times (Blas Lesgourgues & Tram (2011a)) but can maintain accuracy to 0.01% (Blas Lesgourgues & Tram (2011b)). We were thus able to take CLASS simulations as the actual perturbations or anisotropies that would result from a given set of cosmological parameters and initial conditions, and compare them to our expectations based on analytical results. For all simulations we used a standard ΛCDM model with parameters chosen to fit the Planck data. In calculations of the temperature power spectrum we included only the contribution of $\Theta_0 + \Psi$ to justify our direct comparisons with the monopole oscillation.

5. Results and Discussion

We first ask whether primordial perturbations in the temperature monopole, corrected by the Sachs-Wolfe effect to $\Theta_0 + \Psi$, behave as $\cos(kr_s)$, as we would expect if it were described by the first term in the tight coupling solution. Shown in Figure 2 is a CLASS simulation of temperature monopole perturbations, obtained by extracting the values for many k-modes at a single time, in this case approximately the time of recombination. On the left are the original values, and on the right we have eliminated the effects of diffusion damping by dividing by $D(k) = e^{-k/k_D}$ where k_D here is 24.5, chosen to give an approximately constant amplitude to the oscillations (Hu & White (1997)).

Comparing the locations of the peaks and troughs of the undamped monopole to $n\pi$, we calculate the phase shift $\phi = n\pi - kr_s$. To gain additional data points, we can compare the "zero points" of the perturbations, where the second derivative of the curve is zero, to values of $n\pi + \frac{\pi}{2}$. This phase shift is shown as a function

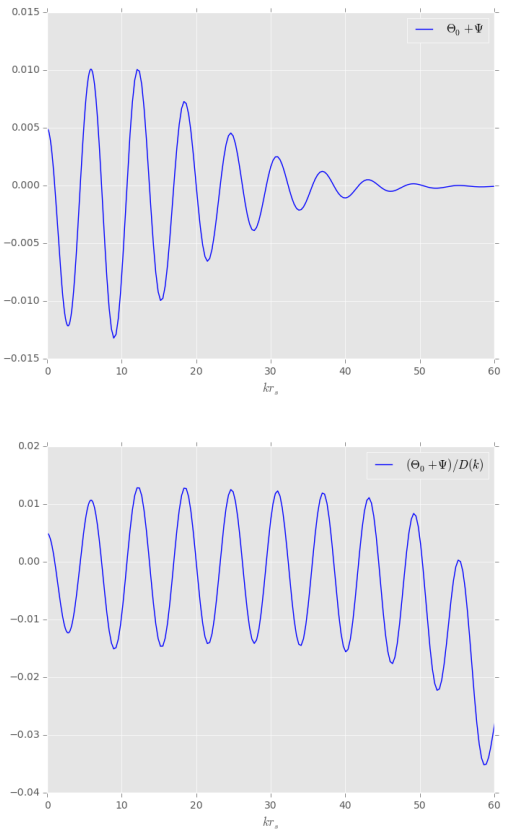

Fig. 2.— Top, temperature monopole perturbations for wavenumbers k at recombination; bottom, perturbations with damping effects removed.

of wavenumber in Figure 3. We can also make a similar analysis of the polarization source term Π, which we expect to have peaks and troughs at $kr_s = n\pi + \frac{\pi}{2}$. The polarization perturbations and their phase shift are shown in Figure 4.

We notice several things about the individual phase shifts of temperature and polarization: first of all, the temperature shift is consistently positive, while the polarization shift centers near 0. However, the curves follow a similar shape, with an initial increase to a maximum when kr_s is between 5 and 10, then a dip followed by a steady increase. It should be noted that trends occuring above $kr_s = 25$ or 30 may not be physically significant, because the tight coupling approximation breaks down at small scales, and moreover, our current measurement capabilities cannot detect

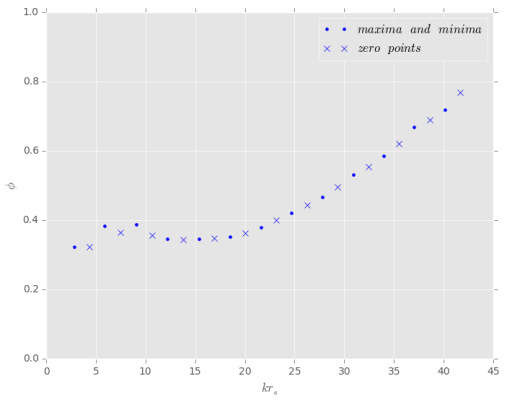

Fig. 3.— Phase shift of temperature perturbations, $\phi_\Theta = n\pi - kr_s$

anisotropies at the corresponding angular scales.

To examine in more detail the relationship between temperature and polarization, we can measure their relative phase shift. If the individual phase shifts for the both source terms were the same or zero, the extrema of the polarization would fall exactly halfway between the temperature extrema. To see how far off from this prediction the real perturbations are, we subtract the locations of polarization extrema from the midpoint between their two adjacent temperature extrema to get the phase shift $\phi_{\Theta,\Pi}$. This relative shift is highest near $kr_s = 25$, when the polarization phase shift is at its minimum while the temperature phase shift has started to rise. If freestreaming translated primordial perturbations directly into present-day anisotropies, we would see exactly the same pattern in the power spectra peaks.

To see how much freestreaming contributes to the phase shift, we examine the projection of perturbations into anisotropies. Based on our reasoning following Equation (22), we expect that extrema of a wavenumber k at recombination project to peaks in the power spectrum at $l = kd_A$. We calculated power spectra and compared their peak locations to peaks and troughs in the perturbations using this conversion. We would expect the difference to asymptote to a constant value at small angular scales, but instead we see it reach a maximum and then begin to decrease. We also note that temperature and polarization are projected differently, with the polarization shift following a smooth curve and the temperature shift displaying oscillations.

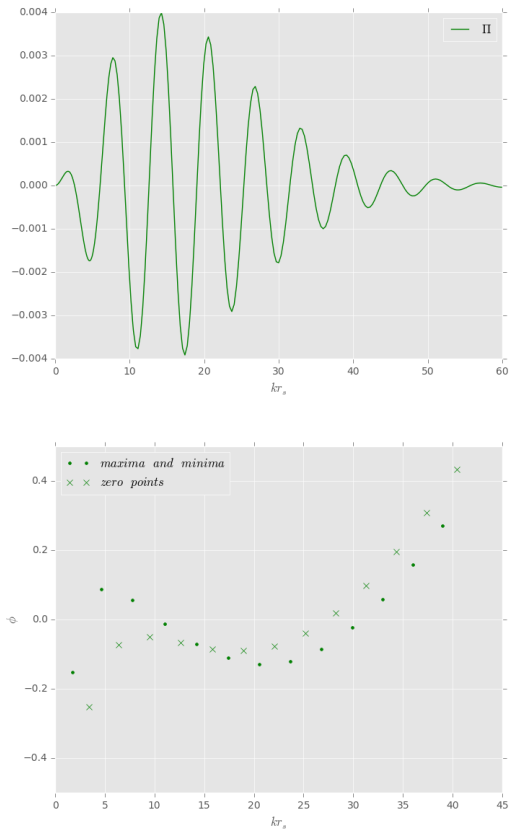

Fig. 4.— Left, perturbations of the polarization source term at recombination. Right, their phase shift $\phi_\Pi = n\pi + \frac{\pi}{2} - kr_s$

6. Conclusion

All of the results shown above are based on a single model of parameters, and it is possible that some effects are model-dependent. Therefore, we cannot draw any decisive conclusions from our observations. For a more complete analysis, the values presented above should be calculated for a suite of models and averaged to eliminate any model-specific effects.

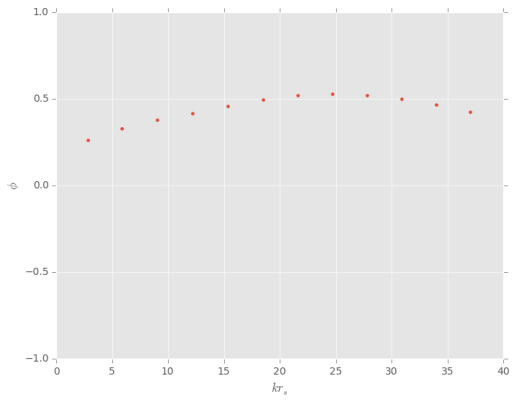

Fig. 5.— How far polarization extrema fall from the midpoints between temperature extrema: $\phi_i = \frac{1}{2}[kr_s(\Theta)_i + kr_s(\Theta)_{i+1}] - kr_s(\Pi)_i$

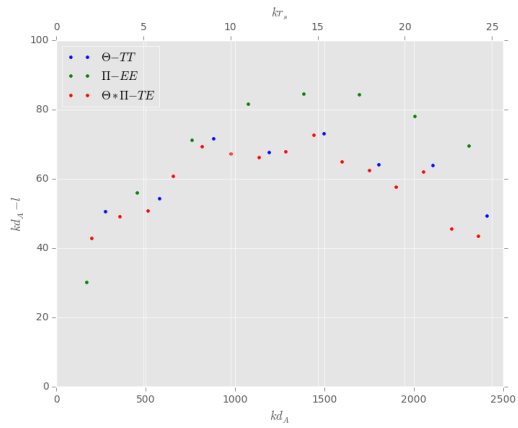

Fig. 6.— Peaks in the temperature, polarization, and TE power spectra are expected to fall near peaks and troughs of the corresponding perturbations at recombination, converted by $l = kd_A$. Here we show $\Delta l = kd_A - l$.

So far, the main conclusion we can draw is that phase shifts in the observed CMB power spectra are affected by both a phase shift in the primordial perturbations and a scale-dependent projection into anisotropies on the sky. While these effects do not sufficiently explain the phase shift observed in the Planck data, they are a first step towards understanding the evolution of CMB anisotropies more deeply.

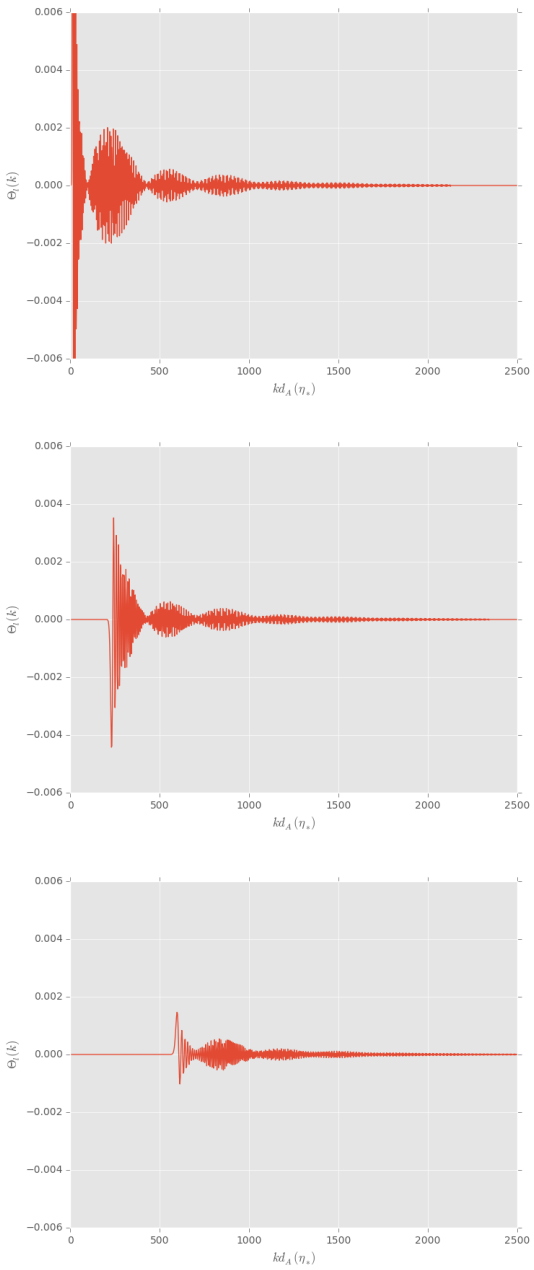

Fig. 7.— Temperature monopole transfer functions $\Theta_l(k)$ for various values of l: top, $l = 12$; middle, $l - 223$; bottom, $l = 582$. The envelope shape mimics the monopole perturbation at recombination. The tight oscillations and the peak near $kd_A = l$ are characteristics of the spherical Bessel function.

REFERENCES

Blas D, Lesgourgues J, Tram T. 2011. The Cosmic Linear Anisotropy Solving System (CLASS). Part II: Approximation schemes. Journal of Cosmology and Astroparticle Physics. 7(2011):34.

Blas D, Lesgourgues J, Tram T. 2011. The Cosmic Linear Anisotropy Solving System (CLASS). Part III: Comparison with CAMB for LambdaCDM. arXiv:1104.2934.

Dodelson S. 2003. Modern Cosmology. San Diego: Academic Press.

Hu W, Dodelson S. 2002. Cosmic microwave background anisotropies. Annual Review of Astronomy and Astrophysics. 40:171-216.

Hu W, Okamoto T. 2004. Principal power of the CMB. Physical Review D. 69.

Hu W, Sugiyama N. 1995. Anisotropies in the Cosmic Microwave Background: An analytic approach. The Astrophysical Journal. 444:489-506.

Hu W, White M. 1997. The damping tail of Cosmic Microwave Background anisotropies. The Astrophysical Journal. 479:568-579.

Planck 2015 results. XI. CMB power spectra, likelihoods, and robustness of parameters.

Seljak U, Zaldarriaga M. 1996. A line-of-sight integration approach to cosmic microwave background anisotropies. The Astrophysical Journal. 469:437.

Zaldarriaga M, Harari D. 1995. Analytic approach to the polarization of the cosmic microwave background in flat and open universes. Physical Review D. 52(6):3276-3287.

This 2-column preprint was prepared with the AAS LaTeX macros v5.2.